be obtained, but with significant deterioration of current-voltage properties: K. L. Hardee and A. J. Bard, *J. Electrochem. Soc.*, **123**, 1024 (1976); **124**, 215 (1977).
(28) D. Dutton, *Phys. Rev.*, **112**, 785 (1958).
(29) R. G. Wheeler and J. Dimmock, *Phys. Rev.*, **125**, 1805 (1962).
(30) (a) R. H. Bube, *Phys. Rev.*, **98**, 431 (1955); (b) D. A. Jenny and R. H. Bube, *ibid.*, **96**, 1190 (1954); (c) J. Camassel, D. Auvergne, H. Mathieu, R. Triboulet, and Y. Marfaing, *Solid State Commun.*, **13**, 63 (1973).
(31) (a) J. J. Lingane and L. W. Niedrach, *J. Am. Chem. Soc.*, **70**, 4115 (1948); (b) A. J. Panson, *J. Phys. Chem.*, **67**, 2177 (1963).
(32) Reference 31a includes redox behavior of Se^{2-}, including the claim that the oxidation product is Se_2^{2-}.
(33) (a) P. L. Allen and A. Hickling, *Trans. Faraday Soc.*, **53**, 1626 (1957); (b) W. M. Latimer, "Oxidation Potentials", 2nd ed, Prentice Hall, New York, N.Y., 1952.
(34) (a) J. F. DeWald, *Bell Syst. Tech. J.*, **39**, 615 (1960); (b) H. Gerischer in "Physical Chemistry", Vol. IXA, H. Eyring, D. Henderson, and W. Jost, Ed., Academic Press, New York, N.Y., 1970, Chapter 5.
(35) T. Watanabe, A. Fujishima, and K. Honda, *Chem. Lett.*, 897 (1974).
(36) (a) Reference 34b, p 485; (b) V. A. Tyagai and G. Ya. Kolbasov, *Surf. Sci.*, **28**, 423 (1971); (c) E. C. Dutoit, R. L. Van Meirhaeghe, F. Cardon, W. P. Gomes, *Ber. Bunsenges. Phys. Chem.*, **79**, 1206 (1975).
(37) Reference 33b, p 174.
(38) "Surface states" located between the valence and conduction band have been detected optically in photoelectrochemical cells employing aqueous electrolytes for SnO_2: H. Kim and H. Laitinen, *J. Electrochem. Soc.*, **122**, 53 (1975); and for CdS: C. E. Byvik, Abstracts, Electrochemical Society Meeting, Washington, D.C., April 1976, No. 238; cf. also S. N. Frank and A. J. Bard, *J. Am. Chem. Soc.*, **97**, 7427 (1975).
(39) T. Inoue, K. Kohayakawa, T. Watanabe, A. Fujishima, and K. Honda, submitted for publication and private communication.
(40) L. Tschugaeff and W. Chlopin, *Ber.*, **47**, 1269 (1914).

Study of *n*-Type Gallium Arsenide- and Gallium Phosphide-Based Photoelectrochemical Cells. Stabilization by Kinetic Control and Conversion of Optical Energy to Electricity

Arthur B. Ellis,[1] Jeffrey M. Bolts, Steven W. Kaiser, and Mark S. Wrighton*[2]

Contribution from the Department of Chemistry, Massachusetts Institute of Technology, Cambridge, Massachusetts 02139. *Received September 27, 1976*

Abstract: We report herein the behavior of *n*-type GaAs- and GaP-based photoelectrochemical cells employing alkaline aqueous solutions of chalcogenide and polychalcogenide ions, X^{2-} and X_n^{2-} (X = S, Se, Te). For GaAs in Te^{2-}/Te_2^{2-} and GaP in Se^{2-}/Se_n^{2-} or Te^{2-}/Te_2^{2-}, the photoanodic dissolution of the GaAs or GaP photoelectrode does not occur; rather, the chalcogenide is oxidized at the photoelectrode. Other combinations of GaAs or GaP photoelectrodes and X^{2-}/X_n^{2-} electrolytes give photoanodic dissolution of the photoelectrode, despite the fact that chalcogenide oxidation is still energetically feasible. The results support the conclusion that kinetic factors, not energetics alone, control whether a given X^{2-}/X_n^{2-} electrolyte will be oxidized at the photoelectrode at a rate which precludes photoanodic dissolution of the electrode. For any case where the photoelectrode is stable, it is possible to sustain conversion of optical energy to electricity. Wavelengths shorter than those corresponding to the band gaps of 2.24 and 1.35 eV for GaP and GaAs, respectively, are effective. Conversion efficiencies for monochromatic light are a few percent, with output voltages of ~0.2–0.45 V at the maximum power output. Sustained conversion is possible because the photoelectrode is stable and also because the electrolyte undergoes no net chemical change, since the substance oxidized at the photoelectrode is reduced at the dark counter electrode.

Much attention is now turning to photoelectrochemical cells[3] as a means of converting optical energy to chemical fuels[4-15] and/or electricity.[16-21] In the preceding paper[20] and elsewhere[16-19] we have established that the photoanodic dissolution of *n*-type semiconductors CdX (X = S, Se, Te) can be quenched by competitive electron transfer from electroactive substances in the electrolyte. Such stabilization of photoelectrodes is also being studied in other laboratories,[21] and it is now quite evident that certain electroactive reagents can be oxidized at irradiated *n*-type electrodes with no other side reactions. For the stabilization of CdX by X^{2-} (X = S, Se, Te), we have further established that the oxidation product (X_n^{2-}) is reducible at the counter electrode to regenerate X^{2-}. The chemistry can be represented as in the reactions

$$A \rightarrow A^+ + e^- \quad \text{(photoanode)} \qquad (1)$$

$$A^+ + e^- \rightarrow A \quad \text{(cathode)} \qquad (2)$$

We have demonstrated that one can exploit such schemes to sustain the efficient conversion of low-energy visible light to electricity, when photoinduced current passes through a load in the external circuit.

A key to further advances in using semiconductor photoelectrochemistry is to elaborate the factors controlling whether the interfacial oxidation of a species A will compete with the photoanodic dissolution of an *n*-type semiconductor. Curiously, for example, CdTe is susceptible to photoanodic dissolution in the presence of S^{2-}, whereas both CdSe and CdS are stable. We showed[20] that S^{2-} oxidation at irradiated CdTe is energetically feasible, but apparently the rate is too slow to completely quench another energetically feasible process corresponding to photoanodic dissolution.

In order to understand the factors controlling interfacial electron transfer at the photoelectrodes, we have pressed to find new examples of quenched photoanodic dissolution. In this paper we report the first stabilization of *n*-type GaP (E_{BG} = 2.24 eV)[22] and GaAs (E_{BG} = 1.35 eV)[23] by the competitive electron-transfer technique using chalcogenide ions as reductants. Both of these *n*-type semiconductors are well known to undergo photoanodic dissolution in aqueous electrolytes.[24-27] We think it noteworthy that these materials are shown to be stabilized by certain chalcogenide ions, but do not themselves contain chalcogenide lattice ions.

Results and Discussion

The sections below detail our characterization of *n*-type GaAs and GaP photoelectrodes in cells employing chalcogenide/polychalcogenide, X^{2-}/X_n^{2-} (X = S, Se, Te) electrolytes. Unless stated otherwise, the solvent is 5.0 M NaOH, and all results have been obtained in cells blanketed under Ar with stirred electrolytes. For three of the six possible combi-

Table I. Behavior of GaZ and CdX in Polychalcogenide Electrolytes[a]

Electrode[b]/ electrolyte	S^{2-}/S_n^{2-}	Se^{2-}/Se_n^{2-}	Te^{2-}/Te_2^{2-}
GaP	Unstable	Stable	Stable
GaAs	Unstable	Unstable[c]	Stable
CdS[d]	Stable	Stable	Stable
CdSe[d]	Stable	Stable	Stable
CdTe[d]	Unstable	Stable	Stable

[a] "Stable" behavior means that for the indicated combination of electrode and electrolyte, enough equivalents of electricity were passed to decompose a substantial fraction of the crystal, yet no weight loss or surface damage was observed (cf. Table III). "Unstable" combinations do not meet these criteria. [b] Single crystals of these *n*-type materials serve as the photoanode and were irradiated with light whose energy exceeded the band gap of the crystal. [c] We do see some oxidation of Se^{2-} at irradiated GaAs, but it is only competitive with GaAs photoanodic dissolution at 0.10 M Na_2Se at 70 °C; see text. [d] Cf. ref 20.

nations of GaAs and GaP, we find that oxidation of the X_n^{2-} occurs at a rate which precludes photoanodic dissolution, Table I. Table I also indicates the stable combinations of CdX and X^{2-}/X_n^{2-}.[20] The results substantiating the claims in Table I for GaAs and GaP will be presented first, and the results of investigations of current-voltage properties, energy conversion efficiency, and open-circuit photopotential will be presented and discussed.

a. Stabilization of GaAs and GaP to Photoanodic Dissolution. According to Memming and Schwandt,[24] irradiation of an *n*-type GaP electrode in alkaline solution results in electron flow such that electrons flow from GaP to the counter electrode. The electron flow at ≤ 10 mA/cm^2 yields photoanodic dissolution of GaP according to the reaction[24,25]

$$GaP + 4OH^- \rightarrow GaO_2^- + P + 2H_2O + 3e^- \quad (3)$$

Meek and Schumaker[25] claim that at higher current densities (≥ 10 mA/cm^2) the reaction

$$GaP + 9OH^- \rightarrow H_2GaO_3^- + HPO_3^{2-} + 3H_2O + 6e^- \quad (4)$$

obtains. We verified, by measuring the weight loss in the GaP, that photoanodic dissolution of GaP in 3 M NaOH obtains with consumption of six holes per GaP at a current density of 12 mA/cm^2. In our hands, the photoanodic dissolution is obvious: prolonged irradiation yields a hole in the GaP crystal.

Analogous studies of the photoanodic dissolution of GaAs have been reported.[26,27] In alkaline media Gerischer[26] reports dissolution according to the reaction

$$GaAs + 10\ OH^- \rightarrow GaO_2^- + AsO_3^{3-} + 5H_2O + 6e^- \quad (5)$$

Unlike CdX anodic dissolution, where the plating out of X quenches the photocurrent, both GaP and GaAs often undergo photoanodic dissolution with stable photocurrents. Williams[28] observed this behavior for GaAs in KCl electrolyte and assumed that GaAs had been stabilized as a photoanode. We found that GaAs photoanodically dissolves in 0.2 M KCl with eventual surface damage and consumption of ~6 mol of holes/mol of GaAs. Thus, stable photocurrent is a deceptive indicator of semiconductor stability. Therefore, we have applied three criteria in assessing photoelectrode stability: (1) photocurrent stability, (2) surface damage, and (3) weight loss in the photoelectrode.

Table I lists the behavior with respect to stability of *n*-type semiconducting GaAs and GaP photoanodes in photoelectrochemical cells employing the listed X^{2-}/X_n^{2-} electrolyte. All experiments consisted of a photoanode and Pt gauze counter electrode in a single vessel. The source and treatment of each GaAs and GaP sample used in this study are given in Table II. For 1 M OH^-/1 M S^{2-}/1 M S (polysulfide) electrolyte, GaAs was shown by irradiation at 633 nm to be unstable by virtue of weight loss and surface damage—an insoluble gray film formed on the electrolyte-exposed surface. This decomposition was observed at a GaAs potential of −0.7V vs. SCE and a current density of ~1.2 mA/cm^2 from irradiation with a 6× beam-expanded He-Ne laser. In the case of GaP, the polysulfide electrolyte absorbs too strongly at $\lambda \leq 500$ nm for GaP (wavelength response onset ~530 nm) to be strongly irradiated. In transparent 1 M OH^-/1 M S^{2-}, however, there is no oxidation of S^{2-} to S_n^{2-} such as is observed for CdS- and CdSe-based cells. Instead, both surface damage and weight loss (corresponding to ~6 mol of electrons/mol of GaP) are observed. In this decomposition the GaP was at −0.22 V vs. SCE and the current density was ~12 mA/cm^2 from irradiation with the visible output from a 200-W Hg lamp. Thus, GaP and GaAs are not stable in sulfide and polysulfide electrolyte, respectively.

For irradiation of either GaP or GaAs electrodes in the presence of a Te^{2-}/Te_2^{2-} electrolyte (0.10 M Te^{2-}, 50 °C), we observed that oxidation of Te^{2-} obtains and completely quenches photoanodic dissolution, Table III. By the procedures described previously,[20] we have established the cell chemistry as in the reactions

$$\begin{aligned} 2Te^{2-} &\rightarrow Te_2^{2-} + 2e^- \\ Te_2^{2-} + 2Te^{2-} &\rightarrow 2Te_2^{2-} + 2e^- \end{aligned} \quad \text{(photoanode)} \quad (6)$$

Table II. Characterization of Electrode Materials

	n-GaP	*n*-GaAs-A	*n*-GaAs-B[a]	*n*-GaAs-C
Supplier	Imanco, Inc., Monsey, N.Y.	Electronic Materials Corp., Pasadena, Calif.	Applied Materials, Santa Clara, Calif.	Crystal Specialities Inc., Moneovia, Calif.
Wafer dimensions	20 mm (diameter) 0.54-mm thick	5 × 5 mm 0.43-mm thick	25 × 30 mm 0.43-mm thick	25 × 25 mm 0.41-mm thick
Dopant	Undoped	Si	Te	Si
Orientation (face exposed)	(111)	(100)	(100)	(111)
Carrier concn, cm^{-3}	3.6–13 × 10^{16}	2–9 × 10^{17}	~10^{17}	3.5 × 10^{18}
Resistivity, Ω-cm	0.27–1.0	0.003	0.003	0.001
Treatment	Etched; smooth, Ga-rich face exposed	Chemically polished on one side	Chemically polished on one side	Chemically polished on one side

[a] This crystal had a 20-μm thick epitaxial layer of Te-doped GaAs grown on a GaAs substrate.

Table III. Stable Combinations of *n*-Type GaZ and Polychalcogenide Electrolytes

Crystal[a]	Initial electrolyte (T, °C)[b]	Crystal before,[c] mol × 10^4	Crystal after,[c] mol × 10^4	Electrons,[d] mol × 10^4	Av i, mA[e]	V_{appl}, V[f]	t, h	Irradiation source[g]
GaP	0.10 M Se^{2-} (63)	6.04	6.04	6.42	1.26	−0.05	13.6	Hg
GaP	0.10 M Te^{2-} (50)	8.02	8.04	3.84	0.51	0.0	10.2	Hg
GaAs	0.10 M Te^{2-} (50)	3.30	3.30	2.26	0.42_5	−0.10	14.2_5	W-X

[a] See Table II for a description of the properties of these crystals. [b] Electrolyte is 5.0 M NaOH and the indicated molarity of Na_2X. The initially colorless electrolyte acquires the color of the polychalcogenide species formed by oxidation of X^{2-} at the photoanode. [c] Moles of crystal determined by weighing the crystal before and after photoelectrochemistry. [d] Moles of electrons passed in the external circuit determined by integrating a plot of photocurrent vs. time. [e] Photocurrent was roughly constant (±10%) throughout the experiments; much of the observed declines can be ascribed to increased absorption by the solution as polychalcogenide species are formed. Current density (mA/cm²) is four times the values shown. [f] Applied bias from power supply in series with photoanode and Pt cathode. Values of 0.0 mean that the two electrodes are short-circuited. Negative values mean that the negative lead of the power supply is connected to the photoanode and represents an electrical load. [g] Hg is a 200-W Hg arc lamp; W-X is a 650-W tungsten-halogen lamp. Both sources are filtered with 18 cm of water to dissipate near IR heat and a Corning 3-73 filter to absorb UV irradiation.

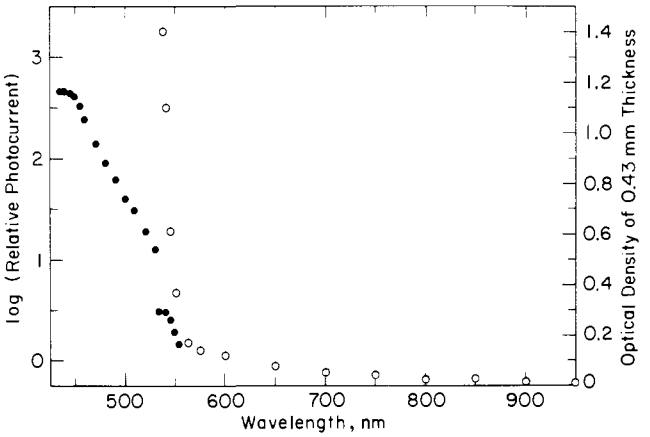

Figure 1. Wavelength response curve for an *n*-type GaP-based photoelectrochemical cell in optically clear 0.1 M Se^{2-} (63 °C) electrolyte. The filled circles represent relative photocurrent *after correction* for light intensity variation (cf. Experimental Section). Open circles represent the absorption spectrum of a polished 0.43-mm thick GaP crystal.

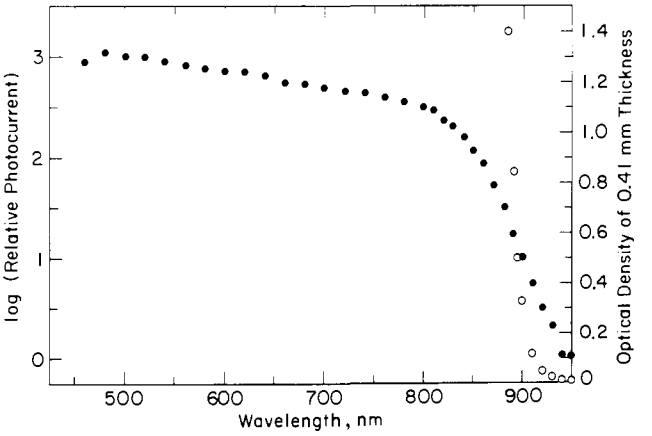

Figure 2. Wavelength response curve for a photoelectrochemical cell employing *n*-type GaAs-B as the photoanode in an optically clear 0.10 M Te^{2-} (50 °C) electrolyte. Symbols are the same as in Figure 1.

$$Te_2^{2-} + 2e^- \rightarrow 2Te^{2-} \qquad \text{(cathode)} \qquad (7)$$

Additionally, we have found that the Se^{2-}/Se_n^{2-} can be used to stabilize GaP, Table III, but under the same conditions (0.10 M Se^{2-}, 63 °C) GaAs is only partially stabilized to photoanodic dissolution. For example, at a current density of 1.6 mA/cm² in 0.1 M Na_2Se at a GaAs potential of −0.80 V vs. SCE, we observe both $Se^{2-} \rightarrow Se_n^{2-}$ oxidation and GaAs dissolution. In the case of GaP stabilization by Se^{2-}, the chemistry is analogous[20] to that shown for Te^{2-} in eq 6 and 7.

b. Wavelength Response. Figures 1 and 2 show the absorption onset and relative photocurrent vs. wavelength for GaP and GaAs, respectively. Consistent with the model for photoelectrochemical cells, the photocurrent onset is at the onset of absorption corresponding to a valence band (VB) to conduction band (CB) transition. For GaP the long, fairly weak absorption tail is a consequence of indirect transitions[29] with low absorptivity. At about ~530 nm there is a strong, sharp increase in absorption, corresponding to the reported direct band gap of 2.24 eV.[22] The wavelength response curve for GaP in either the Te^{2-}- or Se^{2-}-containing electrolyte is consistent with absorption data, in that the onset of photocurrent corresponds closely to the absorption onset. The absorption and photocurrent for GaAs both increase sharply near 930 nm, in accord with the known direct band gap of 1.35 eV.[23]

c. Current-Voltage Properties and Energy Conversion Efficiencies. We have measured the current-voltage properties and energy conversion efficiencies for the three new stable electrode/electrolyte alliances established above.

Potentiostated Current-Voltage Curves. Using the standard three-electrode configuration with a saturated calomel electrode (SCE) as the reference, we have measured the current-voltage behavior of GaP in the Se^{2-}/Se_n^{2-} and Te^{2-}/Te_2^{2-} electrolyte and GaAs in the Te^{2-}/Te_2^{2-} electrolyte. Representative curves are shown in Figures 3 and 4 for GaP and GaAs, respectively, at three different light intensities and in the dark. The key result is that in every case irradiation results in anodic current flow at potentials significantly more negative than the thermodynamically expected potential. For example, the oxidation of Te^{2-} or Te_2^{2-} should occur at −1.05 V vs. SCE[30,31] and for both irradiated GaAs and GaP we see onset of anodic current at ~−1.6 V vs. SCE at the highest light intensity. Likewise, Se^{2-} oxidation, which should occur at −0.95 V vs. SCE[31] is found at ~−1.7 V vs. SCE upon irradiation (224 mW/cm² at 454.5 nm) of an *n*-type GaP photoelectrode. In each of the three electrode/electrolyte combinations we have also measured the potential of the Pt electrode and found it to be invariant at the X^{2-}/X_n^{2-} potential[30,31] for photoelectrode potentials from −1.8 to −1.1 V vs. SCE. The significance of these current-voltage data lies in the fact that one concludes that electrical work can be extracted from the photoelectrochemical cell. The energy conversion efficiencies will be detailed below.

The current-voltage curves (Figures 3 and 4) are influenced by light intensity. In the dark little or no anodic current flow obtains in the potential range scanned, consistent with anodic

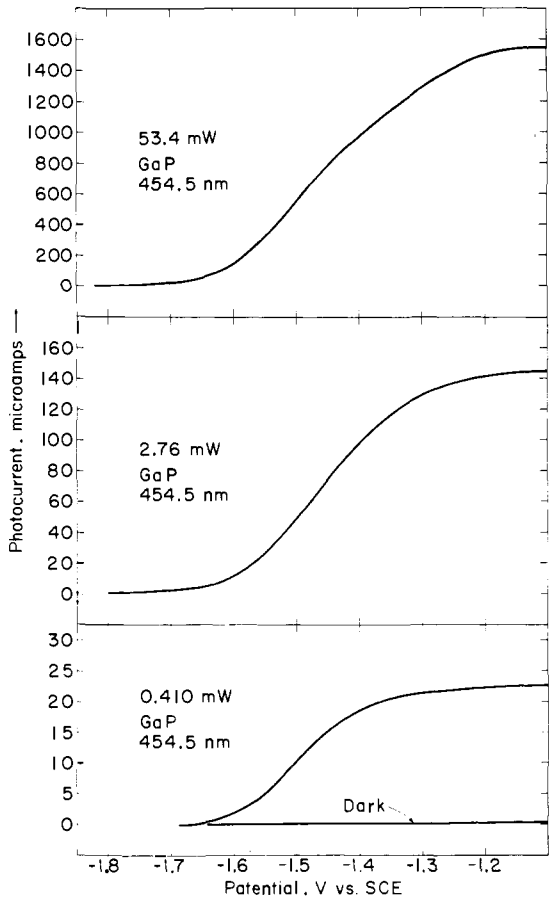

Figure 3. Potentiostated current-voltage curves as a function of light intensity for an *n*-type GaP-based photoelectrochemical cell in 0.10 M Te^{2-} (50 °C). The dark Pt potential was −1.12 V vs. SCE for any bias, and the sweep rate was 2 mV/s. The unexpanded 454.5-nm line of an Ar ion laser was the light source.

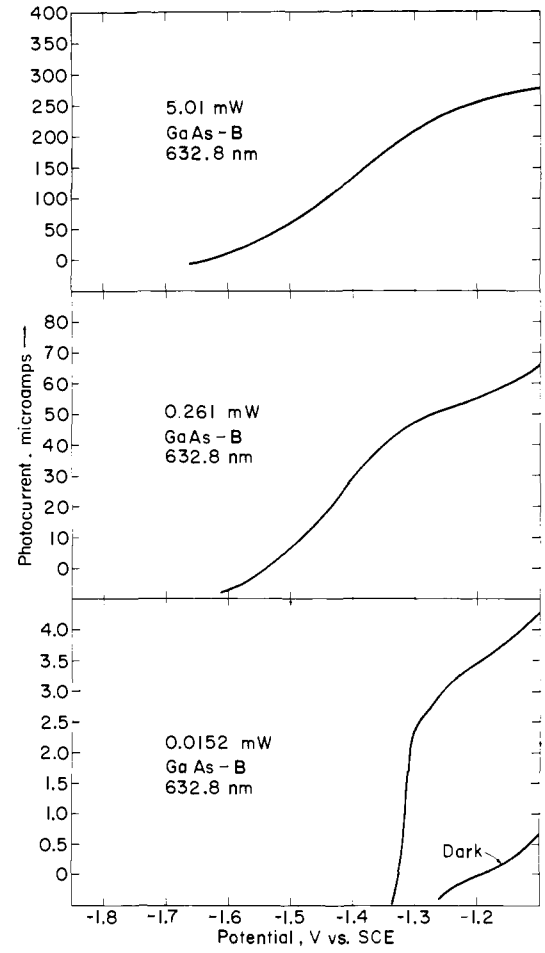

Figure 4. Potentiostated current-voltage properties (cf. Experimental Section) as a function of light intensity for a photoelectrochemical cell employing *n*-type GaAs-B in 0.1 M Te^{2-} (50 °C). The Pt dark potential was always at −1.10 V vs. SCE, and the sweep rate was 2 mV/s. Irradiation source was the unexpanded beam of a He-Ne laser, 632.8 nm.

current flow as a consequence of photogenerated holes, h^+.[3] At low light intensity the onset of anodic current is not as negative as at a higher light intensity. At low light levels the maximum photocurrent is approximately proportional to light intensity. But at the highest light intensities we do see some saturation of the photocurrent, and moreover, the rise of anodic photocurrent with increasing bias is not as steep as at the lowest intensity. Similar trends with variation of light intensity have been found for CdX in X^{2-}/X_n^{2-} electrolytes.[16-20] The more negative onset for the photoanodic current with increasing light intensity reflects the expected[3] dependence of photopotential on light intensity.

Energy Conversion Efficiencies. The facts that (1) the GaAs and GaP can be stabilized to anodic dissolution by competitive electron transfer from certain chalcogenide ions, (2) the oxidation product is reducible at the dark cathode, and (3) oxidation of the chalcogenide occurs at the photoelectrode at significantly more negative potentials than thermodynamically possible point to the conclusion that the GaAs- and GaP-based cells should be able to sustain the conversion of light to electricity.

To determine the energy conversion efficiencies of the GaAs- and GaP-based cells, we have determined current-voltage curves using a variable power supply in series in the external circuit with the negative lead attached to the photoelectrode and the positive lead attached to the Pt cathode. In this configuration the power supply represents an electrical load, since the photocurrent flows against the power supply. The power output of the cell in watts is just the photocurrent in amps times the potential in volts read from the power supply. We have used this technique[16-20] to measure power output, and it is equivalent to measuring the power output using a variable resistor in the external circuit where the output is simply (photocurrent)^2 × resistance. Irradiating with light of band-gap energy, E_{BG}, one could ideally hope for 100% conversion of optical to electrical energy. This would require a quantum efficiency for electron flow, Φ_e, of unity at an output potential, E_V, equal to E_{BG}. In general for band-gap irradiation efficiency is $\Phi_e(E_V/E_{BG})$. Current-voltage data for the stable electrode/electrolyte combinations are set out in Table IV.

All of the current-voltage curves from which the data in Table IV were extracted were obtained in electrolytes where about 20% of the initial X^{2-} concentration had been converted to X_n^{2-}. For example, an initially clear 0.1 M Te^{2-} solution was converted to a dark purple ~0.01 M Te_2^{2-}/0.08 M Te^{2-} solution before obtaining current-voltage curves. The data are not corrected for solution absorption (<10%) or reflection from glass surfaces. For the small (~1-mm) path lengths used, the Se^{2-}/Se_n^{2-} and Te^{2-}/Te_2^{2-} solutions are essentially transparent to visible light.

Percentage energy conversion efficiency is derived from curves like those shown in Figure 5, using the equation

$$\eta = \frac{(\text{photocurrent at } E_V)(E_V)(100)}{(\text{power in from light})} \quad (8)$$

The maximum energy conversion efficiency for all three stable electrode/electrolyte combinations is roughly the same, 1-4%, over a wide range of light intensities. These numbers are quite respectable, although not as good as the 5-10% routinely ob-

Table IV. Conversion of Optical to Electrical Energy for GaZ-Based Photoelectrochemical Cells

Crystal[a]	Electrolyte[b] (T, °C)	λ, nm[c]	Power in,[d] mW/cm²	Max power out,[e] mW/cm²	η_{max}, %[f]	V at η_{max}, V[g]	Φ_e at η_{max}[h]	Φ_e max[i] (V_{appl}, V)
GaP	0.10 M Se^{2-} (63)	454.5	0.540	0.0116	2.15	0.35	0.17	0.19 (0.05)
			4.24	0.0848	2.0	0.40	0.14	0.17 (0.05)
			11.8	0.214	1.8	0.40	0.12	0.17 (0.05)
			224	2.16	0.96	0.45	0.06	0.10 (0.05)
GaP	0.10 M Te^{2-} (50)	454.5	1.64	0.0180	1.1	0.25	0.12	0.16 (0.30)
			11.1	0.106	0.95	0.25	0.10	0.15 (0.30)
			210	1.13	0.54	0.25	0.06	0.09 (0.30)
GaAs	0.10 M Te^{2-} (50)	632.8	1.89	0.071	3.8	0.20	0.54	0.37 (0.05)
			32.2[s]	1.14	3.5	0.20	0.57	0.35 (0.05)
			655	3.56	0.54	0.20	0.09	0.09 (0.05)

[a] Cf. footnote *a*, Table III. [b] The concentration of polychalcogenide in these solutions is about 0.01 M; data is uncorrected for solution absorbance, but the path length from vessel wall to photoanode was kept small (~1 mm) to minimize the error. [c] Unexpanded beam from Ar ion (454.5 nm) or He-Ne (632.8 nm) laser. [d] Light intensity was measured with a Tektronix J16 digital radiometer. [e] Calculated as the product of photocurrent and voltage when the power supply serves as an electrical load (cf. footnote *f*, Table III). [f] Maximum efficiency for the conversion of optical to electrical energy: (max power out/power in) × 100. [g] Output voltage at which the maximum conversion efficiency occurs. [h] Quantum yield for current flow at maximum conversion efficiency; this value represents the number of electrons flowing in the external circuit per number of photons incident on the photoanode. [i] This is the maximum yield and the applied bias at which it occurs.

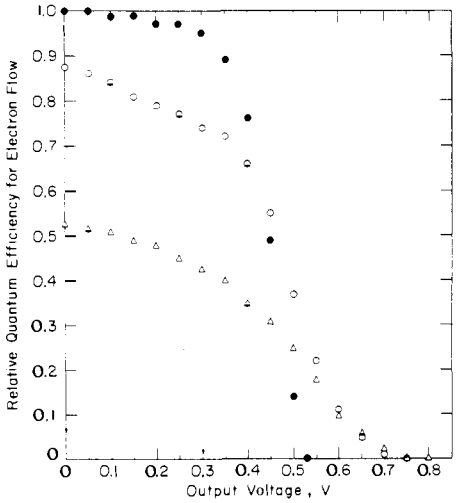

Figure 5. Current-voltage curves for an *n*-type GaP-based photoelectrochemical cell in 0.1 M Se^{2-} (63 °C) electrolyte. Optical to electrical energy conversion efficiencies are obtained from curves like these (cf. Experimental Section); data from this figure are summarized as the first set of entries in Table III. The filled circles (●) represent current-voltage behavior for a power input of 0.54 mW/cm², open circles (○) for 11.8 mW/cm², and triangles (▲) for 224 mW/cm², all at 454.5 nm. The absolute current at 0.0 output voltage and 0.54 mW/cm² input power is 0.0093 mA (Φ_e = 0.19), and this has been set to 1.00. Current at other output voltages at this light intensity is simply the indicated fraction of 0.0093 mA.

served for the stable CdX/(X^{2-}/X_n^{2-}) combinations. The output voltage at maximum energy conversion efficiency, η_{max}, is largest for the GaP/(Se^{2-}/Se_n^{2-}) system and increases from 0.35 to 0.45 V over the intensity range shown in Table III. Lower values of E_V at η_{max} for the GaP/(Te^{2-}/Te_2^{2-}) and GaAs/(Te^{2-}/Te_2^{2-}) combinations were less sensitive to increased light intensity.

The curves shown in Figure 5 and others used to generate the data in Table IV are point-by-point curves, where the photocurrent was allowed to equilibrate before the point was recorded. For all light intensities in Table IV the photoelectrode is stable and the energy conversion efficiencies given can be sustained. Table III, in fact, gives the time scale on which sustained constant conversion of light to electricity has actually been maintained. We anticipate no deterioration of properties in extended duration experiments.

The data in Figure 5 and Table IV show that light intensity does influence energy conversion, but no significant loss in efficiency is found up to ~10 mW/cm² incident optical power. The photocurrent saturation (lower values of Φ_e) reflected in the curves in Figures 3-5 for the higher light intensities is only partially offset by the increased value of E_V. At this point, though, the important fact is that even at >200 mW/cm² incident optical power, there are still reasonable values of Φ_e, η_{max}, and E_V at η_{max}.

d. Energetic and Kinetic Factors Controlling Interfacial Electron Transfer. In this section we wish to refer to the essence of the model[3] for *n*-type semiconductor photoelectrodes and provide evidence that the S^{2-}, Se^{2-}, or Te^{2-} oxidation is energetically feasible at GaAs or GaP photoanodes. The evidence shows further that kinetic factors must control whether this interfacial electron-transfer process will compete effectively with anodic dissolution.

Oxidation of an electroactive substance, X^{2-}, at an irradiated *n*-type semiconductor is energetically feasible, if the potential of the photogenerated holes (h^+) is such that the electron transfer from X^{2-} is exoergic. That is, if the redox potential of the X^{2-}/X_n^{2-} couple, E_{redox}, is more negative than the h^+ potential, then transfer is possible. Fast rates of interfacial electron transfer are expected when the E_{redox} level is near the h^+ position.[3,20] In the ideal case, the position of h^+ will be just the position of the valence band at the surface, E_{VB}. Since we know E_{redox} for S^{2-}/S_n^{2-}, Se^{2-}/Se_n^{2-}, and Te^{2-}/Te_2^{2-} to be −0.70, −0.95, and −1.05 V vs. SCE, respectively, we can use the E_{VB} position to determine whether interfacial oxidation is a reasonable expectation.

We have used[20] open-circuit photopotential, current-voltage curves, and differential capacitance techniques[32] to locate the position of the conduction band at the surface, E_{CB}, and knowing the band gap, E_{BG}, we can then locate E_{VB}. Plots of open-circuit photopotential, E_V, against light intensity for GaAs and GaP in X^{2-}/X_n^{2-} electrolytes are given in Figure 6. The highest value of E_V should allow evaluation of E_{CB}, with $E_{CB} - E_{redox} = E_V(max)$. Unfortunately, we do not see a limiting value of E_V with the light sources available, and we can consequently only place limits on the band positions.

An independent measure of E_{CB} can be made from plots of differential capacitance, C, against electrode potential.[32] A plot of $1/C^2$ vs. electrode potential will be linear, and it is believed that the line intercepts the potential axis at E_{FB}.[32] We have made a determination of E_{FB} by this technique for GaAs in the three X^{2-}/X_n^{2-} electrolytes, and the value is $E_{FB} \approx E_{CB} = -1.5 \pm 0.2$ V vs. SCE. This is the same as that obtained

previously[33] at pH 14 in the absence of the X^{2-}/X_n^{2-} species.

The value for GaP has also been determined previously at pH 14,[33] but we were unsuccessful in obtaining a good plot of $1/C^2$ vs. electrode potential in any electrolyte. Thus, we will use the literature value of $E_{FB} \approx E_{CB} = -2.2$ V vs. SCE for GaP.[33] We will *assume*, as found here for GaAs, that the E_{CB} value for GaP is independent of whether the electrolyte contains the added X^{2-}/X_n^{2-} electrolyte. For all three CdX electrodes we found[20] that the X^{2-}/X_n^{2-} electrolytes shifted the value of E_{CB} more negative by a value of ~0.5 V compared to the NaOH electrolyte. The lack of this shift with GaAs may reflect the absence of a strong X^{2-}/X_n^{2-} interaction with the electrode surface, which does not contain a chalcogenide lattice ion.

The band positions of GaAs and GaP and the values[30,31] of E_{redox} for X^{2-}/X_n^{2-} are shown in Scheme I. The band positions E_{CB} and E_{VB} are obtained from the differential capacitance measurements. We see that the E_V values for GaAs shown in Figure 6 agree fairly well with the separation of the GaAs E_{CB} and the position of X^{2-}/X_n^{2-}. That is, the E_V values, which do tend to level off with the highest light intensity, are in accord with the E_{CB} values from the differential capacitance data. For GaP the plot of E_V against log (light intensity) shows no tendency to level off, and we can only say that E_{CB} must lie at least 1.0 V above the X^{2-}/X_n^{2-} E_{redox} level.

Scheme I

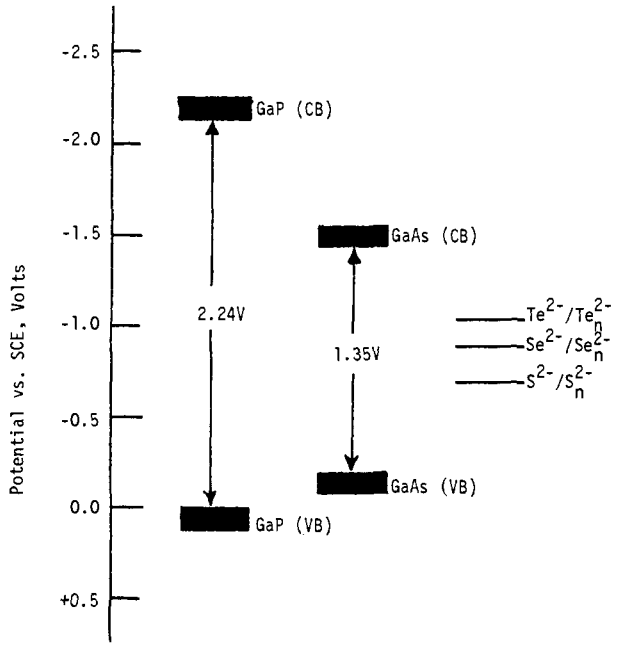

The noteworthy point concerning the information in Scheme I is that in every electrode/electrolyte combination the values of E_{VB} and E_{CB} are significantly below and above, respectively, the E_{redox} value associated with X^{2-}/X_n^{2-}. Thus, oxidation of X^{2-} or X_n^{2-} is energetically feasible in all cases, but the relative rate of the energetically feasible photoanodic dissolution is competitive with the oxidation of the chalcogenide in only one-half of the combinations. The stable combinations of CdX and X^{2-}/X_n^{2-} are included in Table I, and as for GaAs and GaP, we found[20] that in all combinations the E_{VB} position is positive of E_{redox}. Curiously, the E_{redox} systems closest to the E_{VB} position are least capable of fast interfacial electron transfer, and it is the Te^{2-}/Te_2^{2-} couple with the most negative E_{redox} value that can capture photogenerated h^+ fastest. This finding parallels results on CdS exposed to electrolytes having a variable E_{redox}. The ability of a given reducing agent to capture h^+ competitively was found to be dependent on the E_{redox} being significantly more negative than E_{VB}.[21c] If one adopts the notion that h^+ and E_{redox} must be close for fast electron transfer, then surface states between E_{VB} and E_{CB} near E_{redox} could be invoked.[20] We are currently attempting to determine the role of such states in semiconductor-based photoelectrochemical cells.

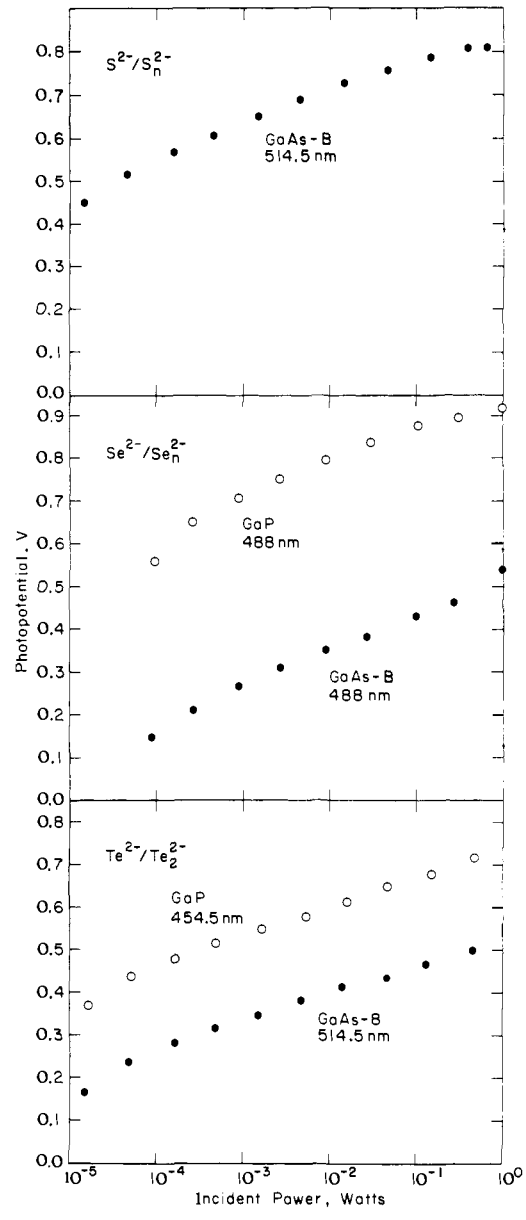

Figure 6. Open circuit photopotentials as a function of incident optical power (cf. Experimental Section) in (a) 1 M S/1 M S^{-2}/1 M OH^- (25 °C), (b) 0.10 M Se^{2-}/5 M OH^- (63 °C), (c) 0.10 M Te^{2-}/5 M OH^- (50 °C). The light source was the unexpanded beam of an Ar ion laser. The intensity is ~50 cm^{-2} times the power shown.

Experimental Section

Materials. The sources and physical properties of the single-crystal *n*-type GaAs and GaP materials are summarized in Table II. The crystals were used as supplied. Electrodes were made by first rubbing gallium–indium eutectic on a face of the crystal, then placing the eutectic-coated face on a glass-encased Cu wire whose end had been coated with conducting Ag epoxy. Ordinary epoxy was used to insulate all exposed metal. For GaP the Ga-rich face was always exposed to the electrolyte; for GaAs the chemically polished face was exposed.

General Procedures. The preparation of electrolytes and electrodes, the cell configuration, and the procedures for measuring current-

voltage curves, quantum yields, photopotentials, wavelength response, and electrode stability have been described previously.[20]

Differential Capacitance Measurements. A Hewlett-Packard 4260A universal bridge was employed for the capacitance measurements. The bias, applied through the bridge leads to the Pt and semiconductor electrodes, was varied in 50-mV steps, and the potential of the anode relative to SCE was monitored on a Data Precision 1450 multimeter. Experiments were performed at 1 kHz in the dark, with a suitable equilibration period after voltage adjustments.

It was found that epitaxially-deposited and single-crystal samples of GaAs gave identical results for E_{FB}, and that the donor densities calculated from the Mott–Schottky slopes were in good agreement with those specified by the suppliers.

For GaP, a Hewlett-Packard 200CD external oscillator was employed in conjunction with the capacitance bridge, and measurements were performed at 200 Hz, and at 1, 2, 10, and 20 kHz. In each case, the slope was too shallow to extrapolate to the E_{FB} intercept, and the measured capacitance was constant to within a few percent over a wide range (>1500 mV) of potentials vs. SCE. It is believed that this result, observed in both chalcogenide and 1 M NaOH electrolytes, is due to the low carrier concentration of our samples, since the variation in capacitance with potential is markedly reduced by decreases in donor density.[34]

Acknowledgment. We thank the National Aeronautics and Space Administration and the M.I.T. Cabot Solar Energy Fund for support of this research. We also acknowledge the assistance of Peter T. Wolczanski in preparing electrode materials.

References and Notes

(1) Fannie and John Hertz Foundation Fellow.
(2) Fellow of the Alfred P. Sloan Foundation, 1974–1976; and Dreyfus Teacher–Scholar Grant Recipient, 1975–1980.
(3) H. Gerischer, *J. Electronanal. Chem.*, **58**, 263 (1975).
(4) (a) A. Fujishima and K. Honda, *Nature (London)*, **238**, 37 (1972); *Bull. Chem. Soc. Jpn.*, **44**, 1148 (1971); (b) A. Fujishima, K. Kohayakawa, and K. Honda, *ibid.*, **48**, 1041 (1975); *J. Electrochem. Soc.*, **122**, 1437 (1975); (c) T. Watanabe, A. Fujishima, and K. Honda, *Bull. Chem. Soc. Jpn.*, **49**, 355 (1976).
(5) M. S. Wrighton, D. S. Ginley, P. T. Wolczanski, A. B. Ellis, D. L. Morse, and A. Linz, *Proc. Natl. Acad. Sci., U.S.A.*, **72**, 1518 (1975).
(6) A. J. Nozik, *Nature (London)*, **257**, 383 (1975).
(7) J. Keeney, D. H. Weinstein, and G. M. Haas, *Nature (London)*, 253, 719 (1975).
(8) W. Gissler, P. L. Lensi, and S. Pizzini, *J. Appl. Electrochem.*, **6**, 9 (1976).
(9) (a) J. G. Mavroides, D. I. Tchernev, J. A.Kafalas, and D. F. Kolesar, *Mater. Res. Bull.*, **10**, 1023 (1975); (b) J. G. Mavroides, J. A. Kafalas, and D. F. Kolesar, *Appl. Phys. Lett.*, **28**, 241 (1976).
(10) K. L. Hardee and A. J. Bard, *J. Electrochem. Soc.*, **122**, 739 (1975); **123**, 1024 (1976).
(11) L. A. Harris and R. H. Wilson, *J. Electrochem. Soc.*, **123**, 1010 (1976).
(12) T. Ohnishi, Y. Nakato, and H. Tsubomura, *Ber. Bunsenges. Phys. Chem.*, **79**, 523 (1975).
(13) G. Hodes, D. Cahen, and J. Manassen, *Nature (London)*, **260**, 312 (1976).
(14) (a) M. S. Wrighton, D. L. Morse, A. B. Ellis, D. S. Ginley, and H. B. Abrahamson, *J. Am. Chem. Soc.*, **98**, 44 (1976); (b) M. S. Wrighton, A. B. Ellis, P. T. Wolczanski, D. L. Morse, H. B. Abrahamson, and D. S. Ginley, *ibid.*, **98**, 2774 (1976); (c) A. B. Ellis, S. W. Kaiser, and M. S. Wrighton, *J. Phys. Chem.*, **80**, 1325 (1976).
(15) J. H. Carey and B. G. Oliver, *Nature (London)*, **259**, 554 (1976).
(16) A. B. Ellis, S. W. Kaiser, and M. S. Wrighton, *J. Am. Chem. Soc.*, **98**, 1635 (1976).
(17) A. B. Ellis, S. W. Kaiser, and M. S. Wrighton, *J. Am. Chem. Soc.*, **98**, 6855 (1976).
(18) A. B. Ellis, S. W. Kaiser, and M. S. Wrighton, *J. Am. Chem. Soc.*, **98**, 6418 (1976).
(19) A. B. Ellis, S. W. Kaiser, and M. S. Wrighton, *Adv. Chem. Ser.*, in press.
(20) A. B. Ellis, S. W. Kaiser, J. M. Bolts, and M. S. Wrighton, *J. Am. Chem. Soc.*, preceding paper in this issue.
(21) (a) G. Hodes, J. Manassen, and D. Cahen, *Nature (London)*, **261**, 403 (1976); (b) B. Miller and A. Heller, *ibid.*, **262**, 680 (1976); (c) T. Inoue, K. Kohayakawa, T. Watanabe, A. Fujishima, and K. Honda, submitted for publication and private communication; (d) D. Laser and A. J. Bard, *J. Electrochem. Soc.*, **123**, 1027 (1976). (e) H. Minoura, T. Oki, and M. Tsuiki, *Chem. Lett.*, 1279 (1976).
(22) C. A. Mead and W. G. Spitzer, *Phys. Rev. Lett.*, **10**, 471 (1963).
(23) R. Barrie, F. A. Cunnell, J. T. Edmond, and I. M. Ross, *Physica*, **20**, 1087 (1954).
(24) R. Memming and G. Schwandt, *Electrochim. Acta*, **13**, 1299 (1968).
(25) R. L. Meek and N. E. Schumaker, *J. Electrochem. Soc.*, **119**, 1148 (1972).
(26) H. Gerischer, *Ber. Bunsenges. Phys. Chem.*, **69**, 578 (1965).
(27) A. Yamamoto and S. Yano, *J. Electrochem. Soc.*, **122**, 260 (1975), and references cited therein.
(28) R. Williams, *J. Chem. Phys.* **32**, 1505 (1960).
(29) W. G. Spitzer, M. Gershenzon, C. T. Frosch, and D. F. Gibbs, *J. Phys. Chem. Solids*, **11**, 339 (1959).
(30) A. J. Panson, *J. Phys. Chem.*, **67**, 2177 (1963).
(31) (a) J. J. Lingane and L. W. Niedrach, *J. Am. Chem. Soc.*, **70**, 4115 (1948); (b) W. M. Latimer, "Oxidation Potentials", 2nd ed, Prentice Hall, New York, N.Y., 1952.
(32) (a) J. F. DeWald, *Bell Syst. Tech. J.*, **39**, 615 (1960); (b) H. Gerischer in "Physical Chemistry", Vol. IXA, H. Eyring, D. Henderson, and W. Jost, Ed., Academic Press, New York, N.Y., 1970, Chapter 5.
(33) (a) M. Gleria and R. Memming, *J. Electroanal. Chem.*, **65**, 163 (1975); (b) W. P. Gomes and F. Cardon, *Z. Phys. Chem. (Frankfurt am Main)*, **86**, 330 (1973).
(34) V. V. Eletskii, Ya. Ya. Kulyavik, and Yu. V. Pleskov, *Sov. Electrochem.*, **3**, 664 (1967).